Scientific Research Publishing

Open Journal of Applied Sciences, 2025, 15(3), 700-714
https://www.scirp.org/journal/ojapps
ISSN Online: 2165-3925
ISSN Print: 2165-3917

Analysis of Axial-Flow and Tilt Aerodynamic Characteristics of Ducted Propellers

Zhongqiu Li, Qi Wang, Tingting Wang

Collage of Aeronautics and Astronautics, Nanchang Hangkong University, Nanchang, China
Email: zhongqiu.lee@163.com

How to cite this paper: Li, Z.Q., Wang, Q. and Wang, T.T. (2025) Analysis of Axial-Flow and Tilt Aerodynamic Characteristics of Ducted Propellers. *Open Journal of Applied Sciences*, **15**, 700-714.
https://doi.org/10.4236/ojapps.2025.153045

Received: March 4, 2025
Accepted: March 18, 2025
Published: March 21, 2025

Abstract

Ducted propellers possess characteristics such as high aerodynamic efficiency, compact structural design, low noise level, and high safety. With the development of electric aircraft, the potential for duct propeller application has become increasingly prominent. In order to further enhance the aerodynamic efficiency of ducted propellers, this study, based on the Navier-Stokes equations, employs the Computational Fluid Dynamics (CFD) method to conduct an in-depth analysis of the aerodynamic characteristics of ducted propellers in the axial flow state and explore their flow characteristics. Firstly, a numerical simulation method suitable for solving ducted propellers is established, and case verification is carried out to ensure the accuracy of the method. Based on this method, the influence laws of different geometric parameters on the aerodynamic efficiency of ducted propellers are analyzed. Based on the simulation results in the axial flow state, a set of parameter combinations with relatively high thrust was selected, and its tilted flight state.

Keywords

Ducted Propeller, Geometric Parameters, Aerodynamic Characteristics

1. Introduction

A ducted propeller is a kind of power device that embeds a propeller inside a circular duct. Due to its excellent aerodynamic efficiency, compact structural design, low noise level, and high safety, it has been widely applied in aerospace and marine equipment such as unmanned aerial vehicles (UAVs), helicopters, and submarines. The presence of the duct effectively suppresses the generation of propeller tip vortices, thereby reducing energy loss. Meanwhile, it generates additional thrust at the lip part, further enhancing the aerodynamic efficiency. In addition, the protective function of the duct reduces the risk of the propeller blades being

damaged in complex environments, enhancing the safety in use [1]. The shielding effect of the ducted structure also helps to reduce the noise level, improving the concealment of the weaponry on the battlefield [2]. However, the complex flow interference between the inner surface of the duct and the propeller tips makes the flow characteristics of the ducted propeller system rather complicated, which significantly affects the aerodynamic efficiency of the ducted propeller [3]. Therefore, an in-depth study of the impact of the geometric parameters of ducted propellers on aerodynamic efficiency is of great significance for expanding their applications in the aerospace field.

A large number of studies both at home and abroad have been carried out based on the Computational Fluid Dynamics (CFD) method regarding the influence of different geometric parameters of ducted propellers on aerodynamic efficiency. Bento studied the aerodynamic characteristics of ducts with different shapes and concluded that the efficiency of circular ducts is higher than that of square ducts [4]. WANG Lei investigated the influence of the bulge at the duct lip on the performance of ducted propellers through numerical simulation and experimental measurement. The results showed that an appropriate bulge can effectively improve the flow distortion at the lip [5]. Han K simulated different duct diameter-chord ratios and lip deflection angles and analyzed their flow mechanisms [6]. XIE Y.F. studied the fillet radius and expansion angle of the duct through numerical simulation and obtained the conclusion that an overly small fillet radius will reduce the duct efficiency [7]. Zou R.H. simulated and studied multiple structural parameters of ducted propellers and analyzed the changes in their lift characteristics [8]. Hu Rui studied different geometric parameters of ducted fans in the hovering state and obtained the influence laws of parameters such as the tip clearance on the fluid flow characteristics inside the duct [9]. Hu Yu studied the influence of the shape of the duct groove on the hovering efficiency of ducted propellers [10]. Li X.H. simulated and analyzed the influence of multiple geometric parameters such as the tip clearance on the flow characteristics of ducted propellers [11].

Most of the above mentioned studies on ducted propellers focus on the influence of geometric factors on flow characteristics, and there is relatively little research content on improving the thrust of ducted propellers. However, in this paper, by analyzing ducted propellers with different parameters, a ducted propeller with relatively high thrust is designed, and the variation law of its thrust in the tilting state is obtained.

2. Simulation Method and Verification

2.1. Numerical Simulation Method

This paper conducts a simulation analysis based on the Multiple Reference Frame (MRF) method. The core of the MRF method is to divide the entire computational domain of the flow field into a rotating domain that contains the propeller blades of the ducted propeller and a stationary domain that contains the duct, as shown in **Figure 1**. The shape of the rotating domain is a cylinder, and its radius is slightly

larger than that of the propeller blades. Inside the rotating domain, the propeller blades are stationary relative to the spatial coordinate system. By assigning a rotational angular velocity to the rotating domain, Think of a resting blade as a moment under unsteady computational conditions [6]. The shape of the stationary domain is also a cylinder. The distances from the inlet and outlet of the flow field to the propeller disk are approximately 8D and 10D respectively, and the distance from the side surface to the boundary of the propeller disk is 5D (where D is the diameter of the propeller).

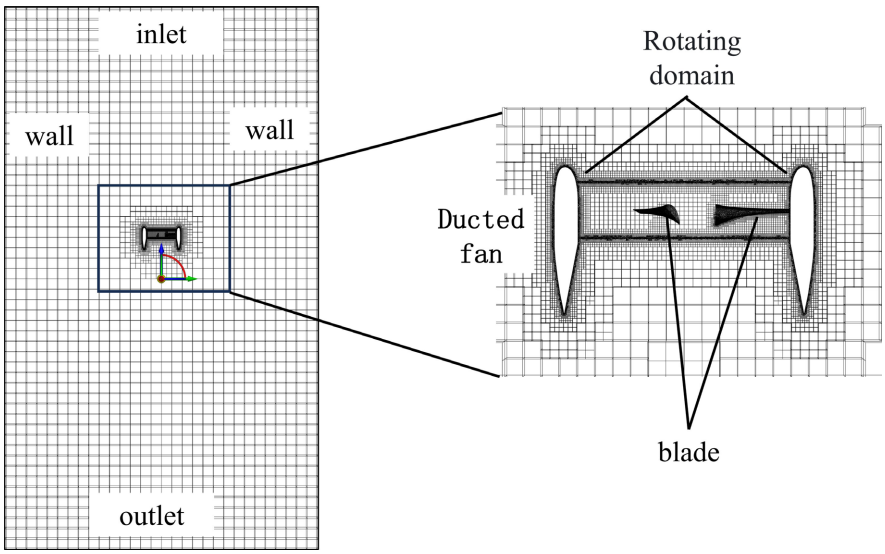

Figure 1. Computational domain partitioning.

When conducting CFD (Computational Fluid Dynamics) simulations, the choice of turbulence model is of great significance. In this paper, the SST-kω turbulence model is adopted. This model is a new shear stress turbulence model established based on the standard k-ω model proposed by Menter [12], integrating the characteristics of the k-ε model. In the boundary layer close to the wall surface, the SST-kω model employs the k-ω model [13], while in the far-field flow region away from the wall surface, it uses the k-ε model. Therefore, the SST-kω model overcomes the drawback of the k-ω model's sensitivity to the incoming flow, combines the advantages of the two turbulence models, and improves the accuracy of the calculation results [14] [15].

2.2. Verification of the Calculation Example

To verify the accuracy of the calculation method, a ducted propeller model was established based on the parameters in the NACA wind tunnel test report. The geometric shape of the ducted propeller is shown in **Figure 2**, and the specific geometric parameters of the duct and the propeller blades can be found in [16].

Boundary conditions were established according to the experimental conditions in [16]. The calculation results were compared with the experimental values, and the comparison results are shown in **Table 1**. The relative errors are all less

than 5%, which is within the acceptable range. This indicates that the calculation method used in this paper has high accuracy.

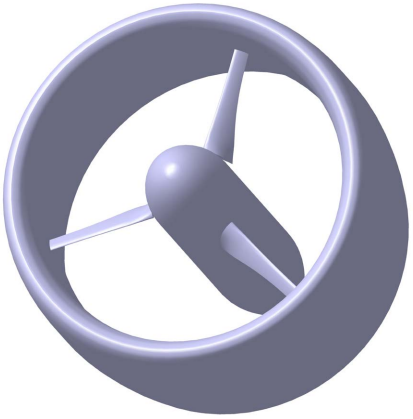

Figure 2. The shape of the ducted propeller.

Table 1. Comparison results between CFD simulation and experimental values.

Parameter value	Simulation value	Experimental value	relative error
Blade thrust/N	62.26	63.97	2.74%
Duct thrust/N	24.61	25.59	3.98%
Total thrust/N	86.87	89.56	3.01%

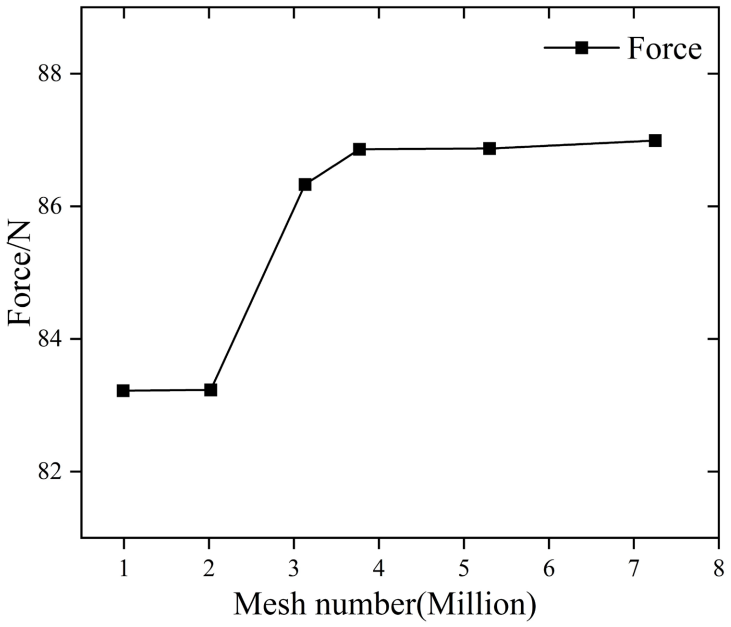

Figure 3. Verification of mesh independence.

2.3. Verification of Grid Independence

To investigate the influence of the number of flow-field grids on the calculation results, based on the geometric model and experimental conditions in [16], the

total thrust of the ducted propeller under axial-flow conditions was calculated. A total of six grid densities (0.99 million, 2.02 million, 3.13 million, 3.77 million, 5.3 million, and 7.25 million) were selected for verification. The same calculation method and boundary-condition settings were applied to the calculation models with different grid densities. The curve of the grid number versus the total thrust of the ducted propeller is shown in Figure 3. When the number of grids is above 3.77 million, the calculation results basically do not change with the increase of the grid number. Therefore, the grid setting with 5.3 million grids was selected for the subsequent calculations.

3. Analysis of the Impact of Geometric Parameters on Ducted Propellers

The aerodynamic characteristics of ducted propellers are significantly influenced by their geometric parameters. Among these, the gap between the propeller tip and the inner wall of the duct, the axial position of the propeller disc within the duct, the angle of the duct's rear section, and the size of the duct's lip radius are particularly important factors affecting the aerodynamic efficiency of ducted propellers. Therefore, this section focuses on simulation analysis of these main parameters of ducted propellers. The geometric model is based on the model in the previous chapter. The simulation conditions are set as follows: the incoming flow velocity is 30.48 m/s in the axial direction of the duct, and the propeller speed is 8000 rpm.

3.1. Influence of the Blade-Duct Gap on the Thrust of Ducted Propellers

The simulation model in this paper is based on the NACA ducted propeller model from the previous chapter, with different ducted propellers formed by changing geometric parameters. This section conducts numerical simulations of the flow field for different blade tip-to-duct inner wall gaps. Based on the propeller disc diameter (D) (381 mm), the blade tip gaps are set at 0.1% D, 0.2%D, 0.5%D, 1.0% D, 2.0%D, and 3.0%D. The variation in thrust of ducted propellers with different blade tip gaps is shown in Figure 4. As the blade tip gap increases from 0.1%D to 3.0%D the total thrust of the ducted propeller first increases and then gradually decreases. When the blade tip gap increases from 0.1%Dto 0.2%D, the thrust generated by the duct remains almost unchanged, while the blade thrust increases by 2.87%, at which point the total thrust of the ducted propeller reaches its maximum value. As the blade tip gap gradually increases from 0.2%D to 3.0%D, the duct thrust decreases by 57.66%, the blade thrust first decreases and then increases before stabilizing, and the total thrust of the ducted propeller decreases by a total of 10.48%.

Figure 5 show the velocity distribution on the X = 0 cross-section of the flow field under different blade tip gaps. It can be seen from this figure that as the blade tip gap increases, the air velocity inside the duct gradually decreases.

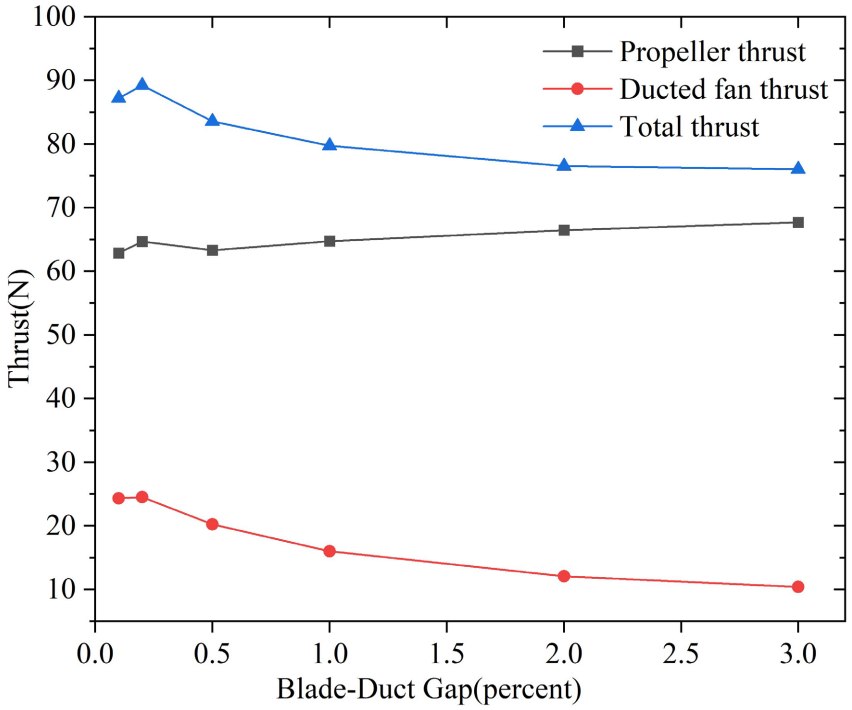

Figure 4. Variation in thrust of ducted propellers with different blade tip gaps.

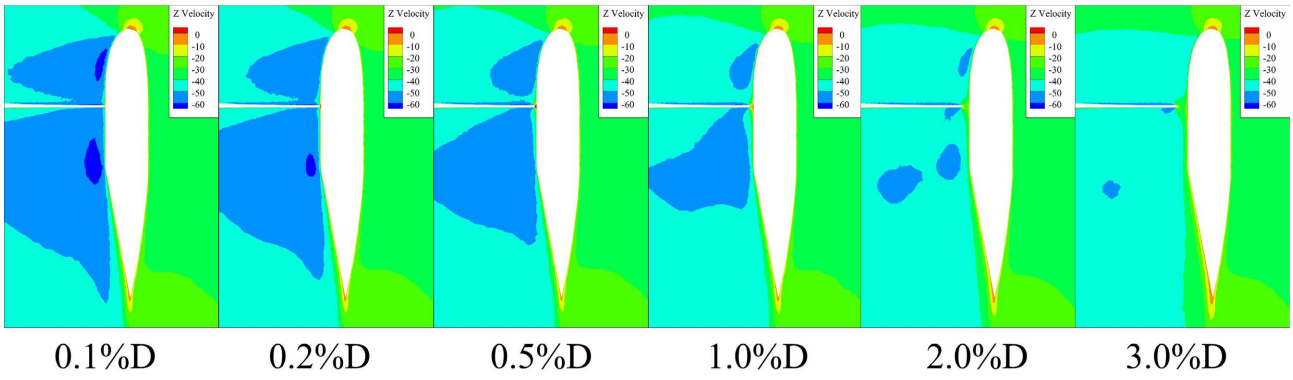

Figure 5. The velocity distribution of the cross-section with different blade tip gaps.

Figure 6(a) shows the variation of surface pressure on the duct with different blade tip gaps. It can be seen from the figure that the negative pressure area and peak value at the front lip of the duct decrease with the increase of the blade tip gap, which leads to a reduction in duct thrust. Figure 6(b) shows the pressure changes along the span of the propeller blade and Figure 6(c) shows the pressure changes of the cross-section at a relative radius of 0.95R. When the blade tip gap increases from 0.1%D to 0.2%D, the blade tip vortex does not change significantly, while the air velocity inside the duct decreases, resulting in an increase in blade thrust. When the blade tip gap increases from 0.2%D to 0.5%D, the increased blade tip gap weakens the duct's ability to suppress the blade tip vortex, leading to a decrease in blade tip thrust and a reduction in overall blade thrust. When the blade tip gap continues to increase from 0.5%D, the blade tip vortex still affects

the pressure distribution at the blade tip, but the effect is weakened. Due to the decrease in axial velocity inside the duct, the local angle of attack of the blade increases, resulting in an increase in blade thrust. When the blade tip gap is greater than 2.0%D, the intensity of the blade tip vortex no longer changes significantly, and the axial velocity near the propeller disc remains almost constant, so the blade thrust begins to stabilize.

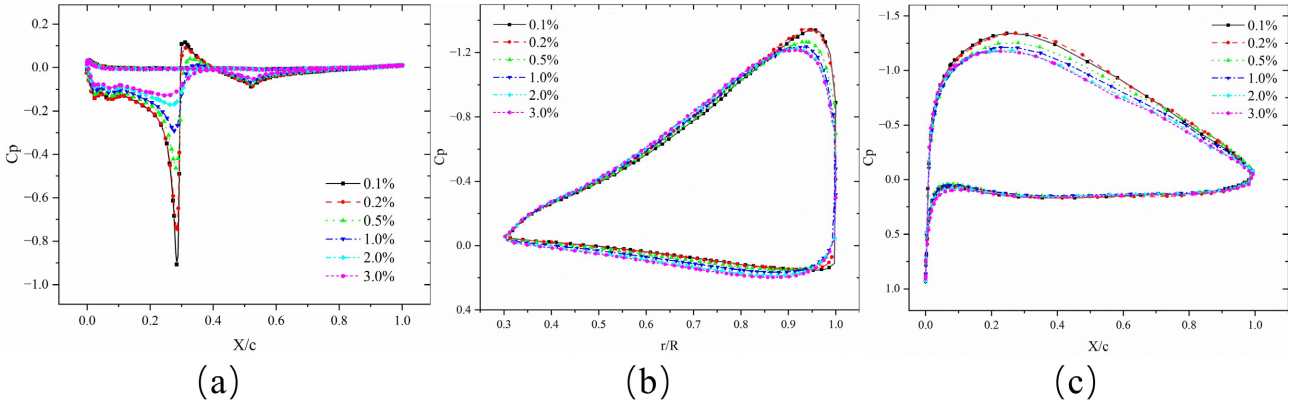

Figure 6. Pressure variations on the surfaces of the duct and blades under different blade tip gaps.

Figure 7 shows the changes of tip vortices under different clearances. It can be seen from the figure that as the clearance increases, the tip vortices gradually strengthen, and the energy leaked from the blade tip thus increases.

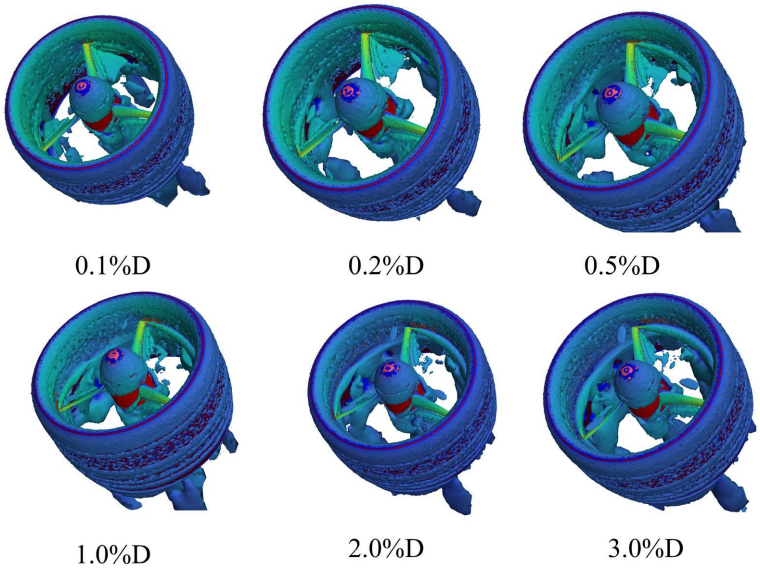

Figure 7. Changes of tip vortices with different clearances.

3.2. Influence of the Angle of the Rear Section of the Ducted Fan on the Thrust of the Ducted Propeller

Numerical simulations were carried out for the two states of contraction and expansion of the rear section of the ducted fan by changing the angle of the rear

section of the ducted fan. The angle variation range is from −10˚ to +15˚ (negative indicates contraction and positive indicates expansion), with a variation unit of every 5˚. Figure 8 shows the variation trends of the thrust of the propeller blades and the ducted fan. When the angle of the rear section of the ducted fan is 0˚, the ducted fan still generates thrust. When the rear section of the ducted fan contracts, the ducted fan generates resistance, and the resistance increases as the contraction angle increases. When the rear section of the ducted fan expands, the thrust generated by the ducted fan gradually increases, reaching the maximum value at around 10˚ of expansion, and then gradually decreases. On the other hand, the thrust of the propeller blades increases as the contraction angle of the rear section increases and decreases as the expansion angle increases. For the total thrust of the ducted propeller, the thrust is the smallest when the rear section contracts by 10˚, and the thrust is the largest when it expands outward by around 5˚.

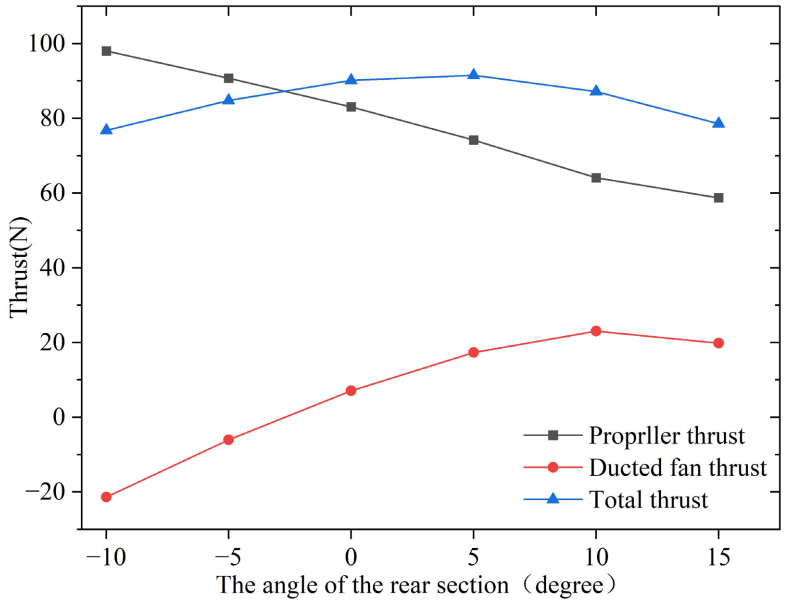

Figure 8. Variation in thrust of ducted propellers with different angles.

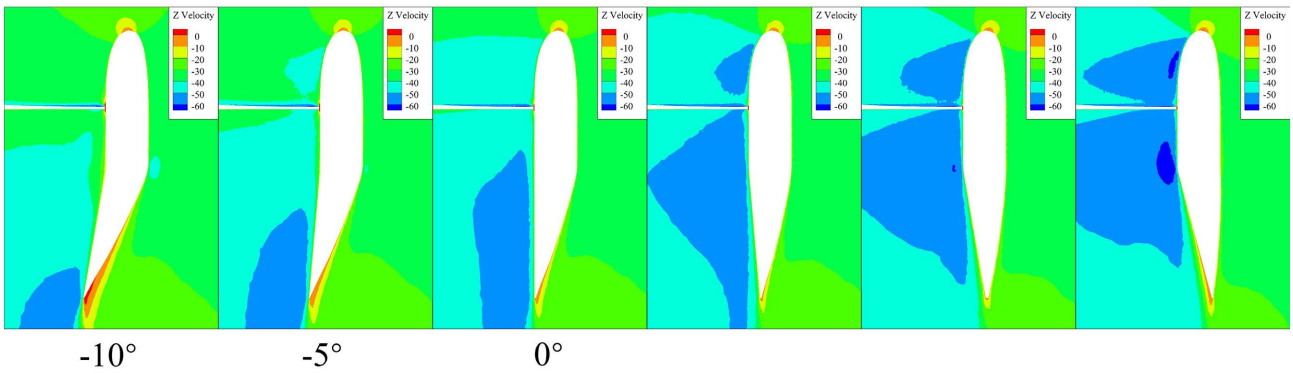

Figure 9. The velocity distribution of the cross-section with different angles.

Figure 9 shows the velocity distribution of the cross-section at X = 0 cross-

section of the flow field under different angles of the rear section. It can be seen from the figures that when the rear section of the ducted fan contracts, the larger the contraction angle is, the lower the airflow velocity will be. When the rear section expands, the larger the expansion angle is, the higher the airflow velocity will be.

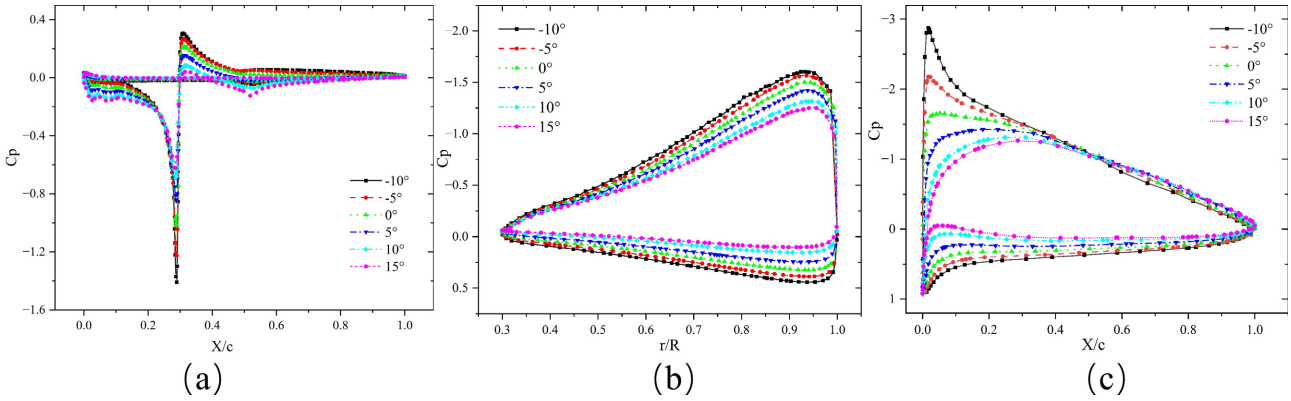

Figure 10. Pressure variations on the surfaces of the duct and blades under different angles.

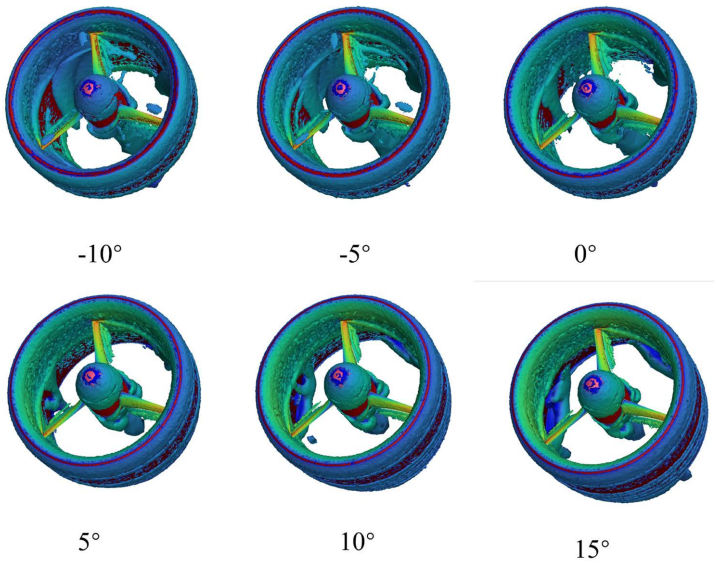

Figure 11. Changes of tip vortices with different angle.

Figure 10(a) shows the pressure changes on the surface of the ducted fan with different angles of the rear section. **Figure 10(b)** shows the pressure changes along the span of the propeller blade and **Figure 10(c)** shows the pressure changes of the cross-section at a relative radius of 0.95R. As can be seen from **Figure 9**, when the rear section of the ducted fan contracts, the area of the negative pressure zone in the front section of the ducted fan is very small, and the surface of the rear section is under positive pressure. Therefore, the ducted fan generates resistance. When the rear section expands, the negative pressure zone increases with the increase of the expansion angle. When the expansion angle of the rear section is 15˚, a relatively large negative pressure zone is generated in the rear section, so the

thrust of the ducted fan decreases again. As the contraction angle of the rear section of the ducted fan increases, the induced velocity inside the ducted fan decreases, the local angle of attack of the propeller blades increases, and the pressure difference between the upper and lower surfaces of the propeller blades increases. Therefore, the thrust of the propeller blades increases. When the rear section of the ducted fan expands, with the increase of the expansion angle, the induced velocity inside the ducted fan continuously increases, the local angle of attack of the propeller blades decreases, and the pressure difference between the upper and lower surfaces of the propeller blades decreases. Therefore, the thrust of the propeller blades decreases.

Figure 11 shows the situation of tip vortices at different angles. It can be seen from the figure that with the change of the angle, the tip vortices change insignificantly. Therefore, the change of the blade thrust is mainly caused by the change of the local angle of attack of the blade.

3.3. Influence of the Position of the Propeller Disk

Through numerical simulations of different positions of the propeller disk in the axial flow state, the variation trends of the thrust of the ducted fan and the propeller blades are obtained, as shown in Figure 12. The propeller disk starts from a position 0.1 L away from the foremost end of the ducted fan (where L is the length of the ducted fan), moves towards the outlet direction, moves 0.1 L unit each time, and ends at the position of 0.6 L of the length of the ducted fan. When the propeller disk is 0.1 L away from the foremost end of the ducted fan, the thrust generated by the ducted fan is relatively small. As the propeller disk moves backward, the thrust of the ducted fan rises rapidly. When it is at the position of 0.5L, the thrust of the ducted fan reaches the maximum value. Compared with that at the position of 0.1 L, the thrust of the ducted fan increases by 265.29%. After exceeding 0.5 L, the thrust of the ducted fan decreases again. The thrust at the position of 0.6 L is 31.51% lower than that at the position of 0.5 L. During this process, the thrust of the propeller blades first decreases and then increases slightly, and the total thrust of the ducted propeller first increases and then decreases. When the propeller disk is at the position of 0.5 L, that is, at the junction of the middle section and the rear section of the ducted fan, the total thrust of the ducted propeller reaches the maximum value. Compared with the minimum value at the position of 0.1 L along the axis of the ducted fan, the total thrust increases by 13.80%.

Figure 13 shows the velocity distribution of the cross-section at X = 0 under different positions of the propeller disk. When the position of the propeller disk is in the front section of the ducted fan at 0.1 L and 0.2 L, due to the strong effect of the tip vortex of the propeller, a stable flow field cannot be formed at the lip of the ducted fan, and the induced velocity at the lip is relatively low. As the position of the propeller disk moves towards the outlet, the influence of the tip vortex of the propeller on the flow at the lip weakens, and the airflow velocity at the lip increases and gradually stabilizes. When the position of the propeller disk enters

the rear section of the ducted fan, due to the increase of the tip clearance of the propeller and the weakening of the inducing effect of the propeller disk, the velocity at the lip of the ducted fan decreases, so the thrust of the ducted fan decreases.

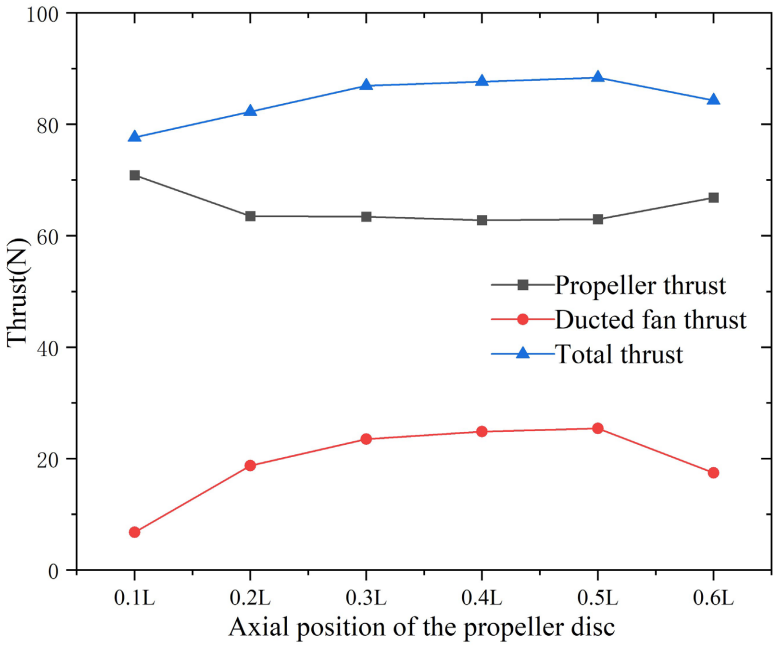

Figure 12. Variation in thrust of ducted propellers with different positions of the propeller disc.

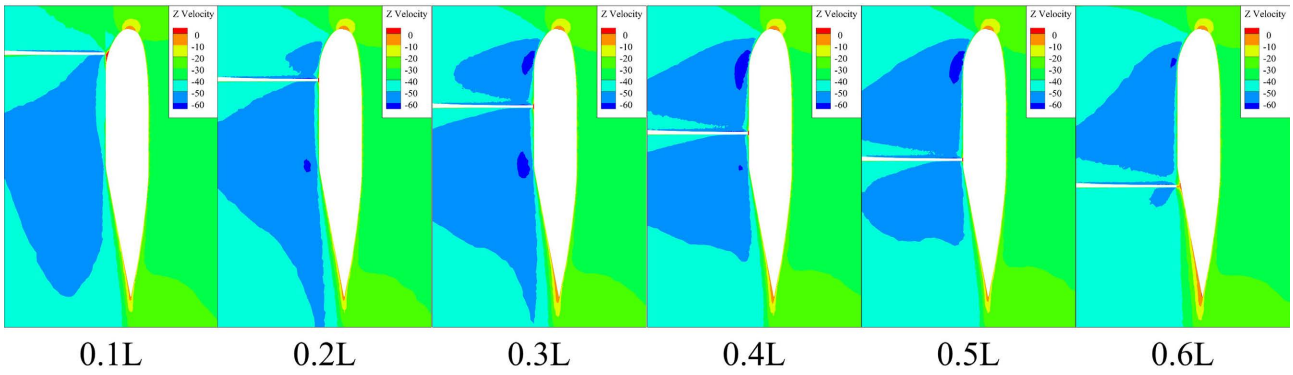

Figure 13. The velocity distribution of the cross-section with different positions.

The pressure changes on the wall of the ducted fan at different positions of the propeller disk are shown in **Figure 14(a)**. It can be seen that when the propeller disk is at the positions of 0.1 L and 0.6 L, both the area and the peak value of the negative pressure zone are relatively small. However, when the propeller disk is in the middle section of the ducted fan, the area of the negative pressure zone is larger, so the thrust of the ducted fan is greater. The pressure changes on the surface of the propeller blades at different positions of the propeller disk are shown in **Figure 14(b)** and **Figure 14(c)**. When the propeller disk is too close to the inlet of the ducted fan, the effect of the tip vortex of the propeller is relatively strong,

and the pressure peak value at the propeller tip decreases. Since the axial velocity inside the ducted fan is relatively low at this time, the local angle of attack of the cross-section of the ducted fan increases, which offsets the thrust loss at the propeller tip. Therefore, the thrust of the propeller blades increases slightly. As the position of the propeller disk moves towards the outlet direction, the effect of the tip vortex of the propeller weakens, and the thrust at the propeller tip increases. However, due to the increase of the axial velocity inside the ducted fan, the local angle of attack of the cross-section of the propeller blades decreases, and the thrust decreases to some extent. When the position of the propeller disk moves backward to the rear section of the ducted fan, the situation is similar to that when it is close to the lip.

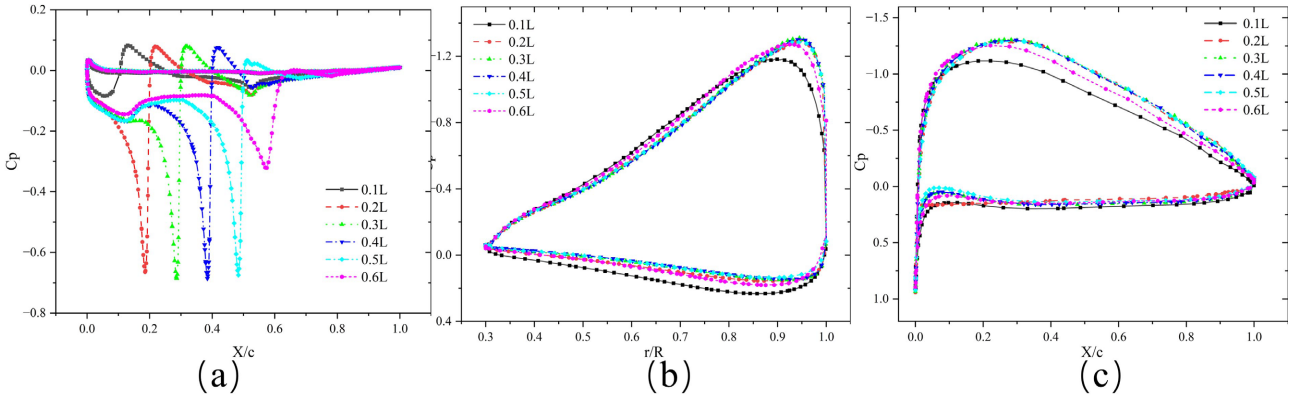

Figure 14. Pressure variations on the surfaces of the duct and blades under different positions of the propeller disc.

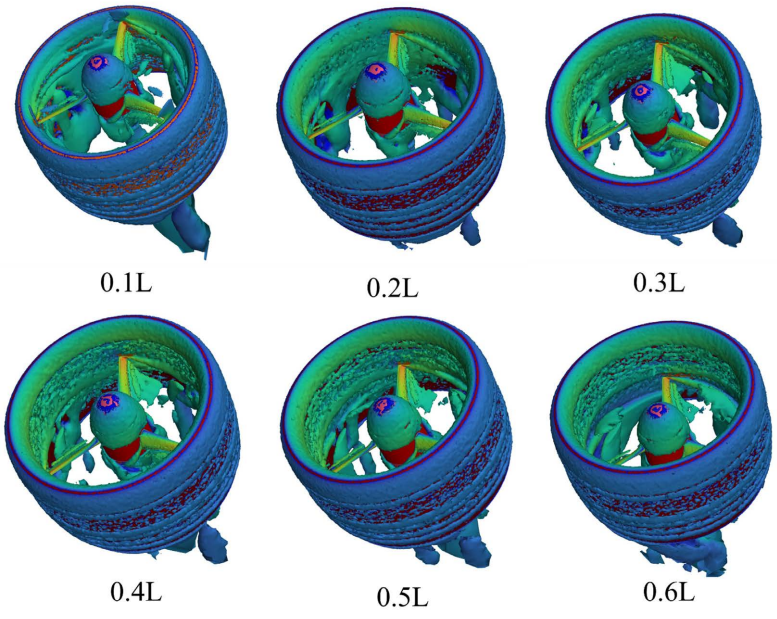

Figure 15. Changes of tip vortices with different positions.

Figure 15 shows the changes of tip vortices at different positions. It can be seen from the figure that when the propeller disk is close to the inlet of the duct and at

the rear section of the duct, the tip vortices are significantly enhanced, so the duct thrust is reduced.

Based on the above research results, a set of geometric parameter combinations was selected, with a gap of 0.12%D, the angle of the rear section expanding outward by 4˚, and the position of the propeller disk at 0.48L. Through simulation analysis, under the boundary conditions described above, its thrust is 92.9N, which is an increase of 6.94% compared to the initial configuration.

3.4. Analysis of the Tilting Characteristics

A simulation analysis is carried out on the tilting characteristics of the ducted propeller. The forward flight state is defined as a tilting angle of 0˚, and the hovering state is defined as a tilting angle of 90˚. The analysis is conducted under the inflow velocities ranging from 5 m/s to 30 m/s. The results are shown in the following figure. As can be seen from Figure 16. For the ducted propeller, when the inflow velocities are 5 m/s and 15 m/s, as the tilting angle increases, the thrust of the propeller blades decreases, while the lift increases. The variation

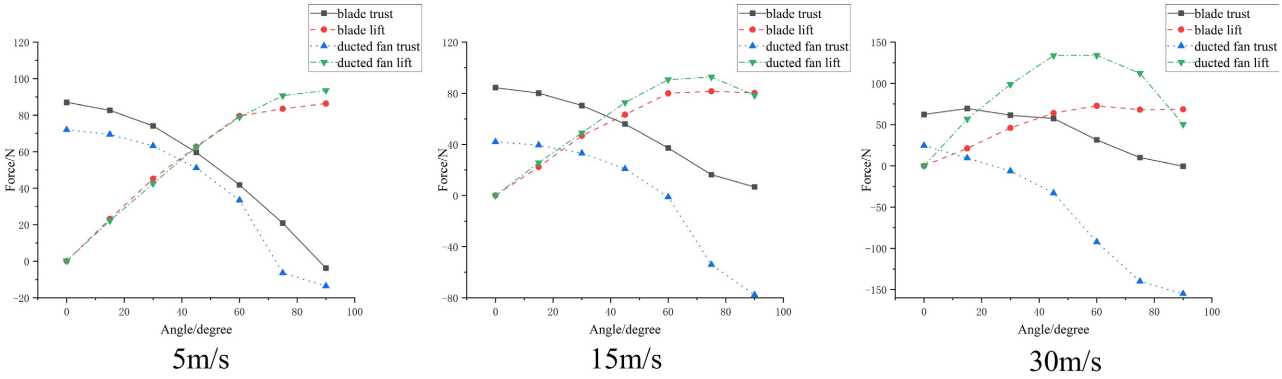

Figure 16. The change of the pulling force in the tilted state.

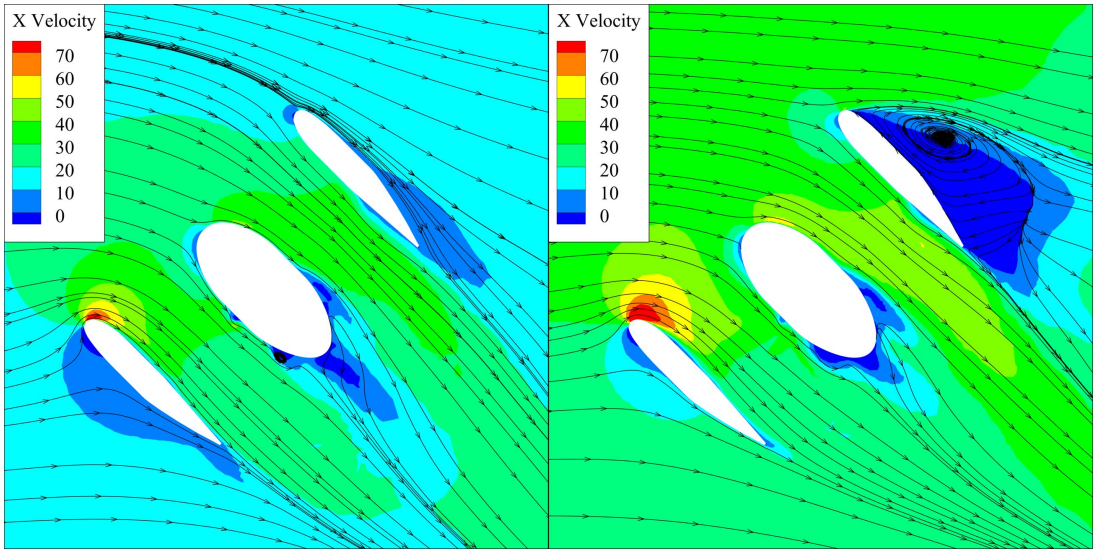

Figure 17. The change of the flow field cross-section velocity during 45˚ tilting.

trend of the ducted fan is basically the opposite. When the inflow velocity is 30 m/s, the lift of the ducted fan shows a trend of increasing first and then decreasing. This is because the inflow velocity is too high. When hovering, the negative pressure zone at the lip of the ducted fan is unstable, resulting in this situation.

Figure 17 shows the cross-section velocity changes at a tilting angle of 45˚. It can be seen that during tilting flight, the rear section of the duct has a good effect of gathering the propeller wake. Therefore, the tilting flight performance of the ducted propeller is better than that of the isolated propeller.

4. Conclusion

Based on the CFD method, this paper studies the influence of the geometric parameters of the ducted propeller on its aerodynamic characteristics in the axial flow state, and analyzes the variation of the thrust force in its tilting state. According to the research results, the propeller tip clearance has a significant influence on the aerodynamic characteristics of the ducted propeller. When permitted by the processing technology, the propeller tip clearance should be as small as possible. When the angle of the rear section of the duct is around 5˚ of outward expansion, the thrust force is the largest. When the position of the propeller disk is in the middle section, the thrust force is relatively large. During the tilting process of the ducted propeller, the incoming flow velocity should not be too large; otherwise, the lift force will decrease.

Conflicts of Interest

The authors declare no conflicts of interest regarding the publication of this paper.

References

[1] Li, H. (2021) Research on the Overall Design and Aerodynamic Characteristics of a Ducted Coaxial Rotor UAV. Ph.D. Thesis, University of Chinese Academy of Sciences.

[2] Deng, Y., Mi, B., Zhan, H. and Cao, F. (2020) Ground Test and Numerical Simulation on Ground Effect of Ducted Propeller System. *Journal of Northwestern Polytechnical University*, **38**, 1038-1046. https://doi.org/10.1051/jnwpu/20203851038

[3] Ji, L.Q. (2017) Research on Key Technologies of Rotor/Ducted Fan Unmanned Helicopter Preliminary Design. Ph.D. Thesis, Nanjing University of Aeronautics and Astronautics.

[4] Bento, H.F., de Vries, R. and Veldhuis, L.L. (2020). Aerodynamic Performance and Interaction Effects of Circular and Square Ducted Propellers. AIAA Scitech 2020 Forum, Orlando, 6-10 January 2020, 1029. https://doi.org/10.2514/6.2020-1029

[5] Wang, L., Su, G.T., Pan, T.Y., Lu, H.N., Zheng, M.Z. and Li, Q.S. (2025) Investigation of Performance Effects and Operational Mechanisms of Lip-Installed Bump on Ducted Fan under Boundary Layer Ingestion. *Journal of Propulsion Technology*, 1-16. https://link.cnki.net/urlid/11.1813.v.20240717.1410.006

[6] Han, K., Bai, J.Q., Qiu, Y.S. and Chang, M. (2022) Aerodynamic Performance and Flow Mechanism of Ducted Propeller with Different Design Variables. *Acta Aeronautica et Astronautica Sinica*, **43**, Article 125466.

[7] Xie, Y.F. and Ge, N. (2024) Researchon Aerodynamic Design of High Altitude High Thrust Ducted Fan. *Machine Building & Automation*, **53**, 87-92.

[8] Zou, R.H., Hu, W.J. and Wang, H.Y. (2024) CFD Simulation of Aerodynamic Characteristics of Ducted Propeller and Analysis of Influence of Structural Parameters. *Fluid Measurement & Control*, **5**, 7-10.

[9] Hu, R., Cao, C.K., Zhan, G.Q. and Zhao, Q.J. (2023) Investigations of the Layout Parameter Influence on the Aerodynamic Characteristics of Ducted Fan. *Flight Dynamics*, **41**, 7-12.

[10] Hu, Y., Zhang, X.P., Wang, Q., Luo, Z.N. and Wang, G.Q. (2025) Improved Design of Hovering Efficiency of Ducted Propeller with Large Blade Tip Clearance Based on Grooved Duct Configuration. *Journal of Aerospace Power*, **40**, Article 20220650.

[11] Li, X.H. (2014) The Impact Analysis of the Aerodynamic Characteristic on Ducted Fan Profile Parameters. Master's Thesis, National University of Defense Technology.

[12] Menter, F.R. (1994) Two-Equation Eddy-Viscosity Turbulence Models for Engineering Applications. *AIAA Journal*, **32**, 1589-1605. https://doi.org/10.2514/3.12149

[13] Guan, J. and Guo, Z. (2013) Numerical Simulations of Low-Reynolds-Number Flows over the E387 Airfoil. *Science Technology and Engineering*, **13**, 7275-7281.

[14] Qiu, Y.S., Bai, J.Q., Li, Y.L. and Zhou, T. (2012) Study on Influence of Complex Geometry Details on the Aerodynamic Performance of High-Lift System. *Acta Aeronautica et Astronautica Sinica*, **33**, 421-429.

[15] Li, X.H., Guo, Z. and Chen, Q.Y. (2015) Numerical Simulation of Ducted Rotor's Aerodynamic Characteristics. *Journal of National University of Defense Technology*, **37**, 31-35.

[16] Goodson, K.W. and Grunwald, K.J. (1962) Aerodynamic Loads on an Isolated Shrouded-Propeller Configuration.